Effects of Deposition Rate on Microstructure of CoCrPt-SiO_2 Granular Longitudinal Media for Tape Applications

Lin Wang, Hwan-Soo Lee, Yueling Qin, James A. Bain, and David E. Laughlin

Data Storage Systems Center, Department of Materials Science and Engineering, Carnegie Mellon University, Pittsburgh, PA 15213 USA

The microstructure of sputtered CoCrPt-SiO_2 media for tape applications was investigated under different deposition rates. Plan-view and high-resolution cross-sectional TEMs were used to observe the media growth morphology and oxide phase separation behavior. Additionally, time-dependent magnetic property measurements were used for switching volume determination. Although plan-view TEM images suggested well-isolated, small grains, cross-sectional TEM images and switching volume measurements revealed magnetic interconnection between the apparent "grains" visible in the plan-view images. When the deposition rate was reduced from 0.28 to 0.05 nm/s, TEM images showed larger features in plan-view, which is consistent with greater time for atomic motion on the surface before burial. It was also observed in cross-sectional TEM images that columnar growth at the higher rate changed to spheres of metal in an SiO_2 matrix at low deposition rate.

Index Terms—**Deposition kinetics, exchange decoupling, granular media, interfacial energy, phase separation, sputtered thin-film magnetic tape media.**

I. Introduction

FOR DECADES, tape, with its unique cost-efficient characteristic due to its volumetric storage density, has served in archival data storage. Innovation in the field has been focused on finding the next-generation high-density, high-performance tape media. Along with candidates proposed in the advanced metallic particle (MP) or advanced metal evaporated (ME) tape media families, sputtered tape media is another, very promising, candidate. Its strength is the ability to support very high densities, as in hard disk drive (HDD) media. The challenges associated with sputtered tape center around the processing challenges of low-temperature and high-rate deposition. For manufacturing purposes, deposition rates of 10 nm/s would be desirable, but such high rates provide some challenges, including realization of the correct microstructure and parasitic heating of the plastic substrate, which is unacceptable.

In both longitudinal and perpendicular recording, magnetic media with an SiO_2 matrix is a promising candidate for obtaining magnetic grain decoupling to reduce media noise without heating or annealing [1]. This type of media is of particular interest in magnetic tape applications, where the low-temperature deposition is paramount to avoid substrate damage.

Thus, this study focuses on the effect of deposition rate in the longitudinal CoCrPt-SiO_2 materials system and the behavior of metal–oxide phase separation. Since two phase segregations must occur during the sputtering deposition process, it is anticipated that the deposition rate may be a crucial deposition parameter and that different deposition rates may produce different metal–oxide phase separation behaviors due to different deposition kinetics and attempts by the system to minimize interfacial energy.

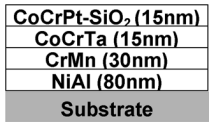

Fig. 1. Samples' stacking layers: substrate/NiAl (80 nm)/CrMn(30 nm)/CoCrTa (15 nm)/CoCrPt-SiO_2 (15 nm).

II. Experiment

Thin films of CoCrPt-SiO_2 (15 nm thick) were produced by RF magnetron sputtering under 10-mtorr Ar gas pressure with different deposition rates by varying the deposition power. The underlayer and intermediate layer stack used was substrate/NiAl(80 nm)/CrMn(30 nm)/CoCrTa(15 nm) obtained by DC magnetron sputtering under 10-mtorr Ar gas pressure on Si substrates covered with a native oxide (Fig. 1). The magnetic properties of these films and their time-dependent behavior were characterized by alternating gradient magnetometry (AGM). Microstructures of these films were examined with plan-view TEM in bright field (BF) and dark field (DF) contrast modes to assess for grain size and orientation. The DF images were obtained by selecting part of the (00.2) polycrystalline diffraction ring with the aperture in diffraction mode. High-resolution cross-sectional TEM in BF mode was also used to characterize media growth morphology.

Two media-layer growth rates are compared in this paper: Media I deposited at 0.28 nm/s for the media layer [target power used was 200 W (Target voltage $=$ 389V)] and Media II deposited at 0.05 nm/s for the media layer [target power used was 50 W (Target voltage $=$ 176 V)]. All underlayers were deposited under a fixed set of conditions that was not varied

Digital Object Identifier 10.1109/TMAG.2006.879644

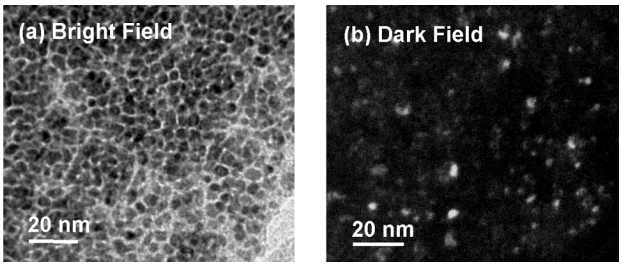

Fig. 2. BF and DF TEM images of Media I sputtered with a media layer deposition rate of 0.28 nm/s.

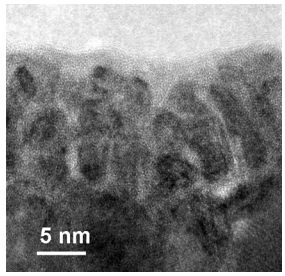

Fig. 3. High-resolution cross-sectional TEM images of Media I sputtered with a media layer deposition rate of 0.28 nm/s. The white contrast region was the SiO_2 phase.

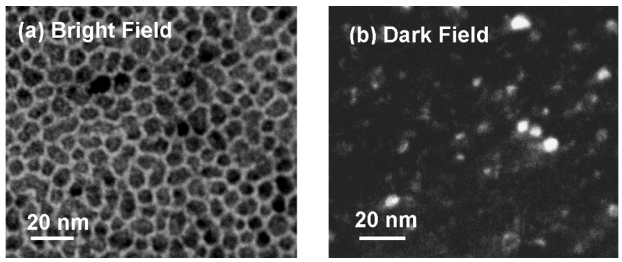

Fig. 4. BF and DF TEM images of Media II sputtered with a media layer deposition rate of 0.05 nm/s.

when the deposition rate of the magnetic layer was changed. The sputtering target for CoCrPt-SiO_2 media layers of Media I and Media II was the same.

III. Results and Discussion

X-ray diffraction patterns of both media (not shown) suggested that both Media I and Media II were 3-D random in their crystalline orientations. While strong in-plane is the desired microstructure in these films, the effect of deposition rates in these samples is still instructive. For samples deposited at a deposition rate of 0.28 nm/s for the media layer using 200-W power (Media I), from the plan-view TEM image, it was found that the grains looked reasonably well separated by the SiO_2 nonmagnetic phase and the visual "grain size" appeared quite small—about 5 nm. This microstructure can be seen in Fig. 2(a).

However, the coercive squareness S^* of this film was 0.79, which was higher than expected and indicated significant magnetic grain coupling, and the coercivity was low (3.1×10^4 A/m, 390 Oe) at a field application rate of 0.1 s/step. Using AGM, we obtained coercivity H_c for various measurement time scales t. We then plotted H_c versus $[ln(f_0 t)]^{0.7}$ according to the analysis described in [2] and [3], which employ the following relationship:

$$H_c(t) = H_0\{1 - [(k_B T/(K_u V))\ln(f_0 t)]^{0.7}\} \qquad (1)$$

where f_0 is the attempt frequency for thermally assisted switching (taken as 10^9 Hz), H_0 is the field required to switch with no thermal assistance, k_B is Boltzmann's constant, T is the absolute temperature, K_u is the anisotropy energy density of the switching unit, and V is the volume of the switching unit that is thermally activated, and we assume that the average misalignment angle in the Sharrock formula is around 45°. From this analysis, H_0 and $k_B T/(K_u V)$ were extracted. Then, we obtained K_u under the assumption that $H_0 = H_k/2$, and, as usual, the anisotropy field H_k is defined by $H_k = 2K_u/(\mu_0 M_s)$.

The results of the time-dependence calculation showed that the stability coefficient $K_u V/(k_B T)$ was about 49 for Media I, with a K_u value of 4.39×10^4 J/m^3, and a cylindrical switching volume with a diameter of 19 nm, in a film thickness of 15 nm. This diameter of switching volume was much larger than the 5-nm apparent grain size shown in the plan-view TEM image, while the K_u was about an order of magnitude lower than what was reported in [4]. We interpret this result as evidence of partial coupling between the randomly orientated grain, which has the effect of lowering the average K_u within a cluster and increasing the apparent switching volume. Of course, if the coupling is only modest, and the individual parts of a coupled cluster can switch independently, then the above analysis cannot be taken as fully quantitative. However, no set of reasonable assumptions within the thermal activation analysis resulted in being able to treat the individual entities seen within Fig. 2(a) as isolated switching volumes.

Both the DF plan-view images in Fig. 2(b) and the high-resolution cross-sectional image in Fig. 3 were consistent with this conclusion. Fig. 2(b) shows regions where several adjacent grains all appear in the diffracting condition, indicating crystallographic registry between these grains. By plan-view TEM examination of the samples with only an NiAl/CrMn/CoCrTa underlayer and intermediate layers, we found that the grain size of CoCrTa was about 20 nm, which is much larger than the visual grain size of the CoCrPt-SiO_2 media layer. In the previous study [5], without SiO_2 in the CoCrPt media, the grain was also around 20 nm in size (although a little bit less than 20 nm). Additionally, Fig. 3 showed that the SiO_2 matrix was discontinuous in the through thickness direction, thus several adjacent grains may come from the same underlayer template grain and still be magnetically interconnected.

For Media II, the deposition rate was lowered to 0.05 nm/s, allowing the SiO_2 phase to have a longer time to segregate and reach equilibrium before burial. As expected, the effects were a larger visual grain size of about 8 nm and much better defined SiO_2 on the boundary (Fig. 4). Given the 2-D random walk nature of the surface diffusion, this effective grain size is somewhat smaller than the expected value of 12 nm, which would be expected from scaling the in-plane feature size with the inverse square root of the deposition rate [6]. Magnetic measurements indicated reductions in S^* consistent with this (to 0.61), but were complicated by increases in the 3-D random nature

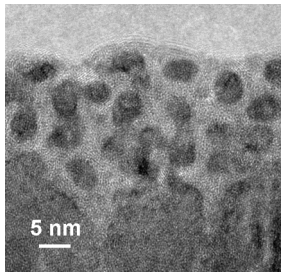

Fig. 5. High-resolution cross-sectional TEM images of Media II sputtered with a media layer deposition rate of 0.05 nm/s.

of the orientation. The coercivity of this film was even lower, at 1.48×10^4 A/m (186 Oe) at a field application rate of 0.1 s/step, and the stability coefficient $K_u V/(k_B T)$ was 34. The calculated diameter of switching volume of Media II was 19 nm, which was consistent with the calculation of Media I.

An important contrast in the film morphology for different deposition rates was seen from the high-resolution cross-sectional TEM examination. Fig. 5 is a typical cross-sectional profile of Media II's CoCrPt-SiO_2 media layer. Comparing with Fig. 5, Media II was less columnar in its growth morphology. The cross-sectional TEM image showed that the SiO_2 network pattern was also regular at the thickness dimension. Thus, incorporating it with the plan-view image of Media II in Fig. 4, we can tell in a 3-D image perspective that the SiO_2 was formed in a shell pattern around the Co-alloy spheres at low growth rates. As with Media I, Media II's magnetic properties also indicate coupling between the small regions.

Analysis of this change in morphology can shed some light on the kinetics of the deposition and segregation process. From a thermodynamic perspective, spherical shapes minimize surface per unit volume. Slow deposition might be considered closer to equilibrium, so spheres might be obtained in this limit.

However, the nucleation behavior must also be considered, since the SiO_2 and CoCrPt must repeatedly nucleate through the film thickness to produce cylindrical grains. We are assuming that all diffusion takes place in the surface layer during deposition. In this model, slower growth appears to favor new nucleation events over attachment to existing grains. This might be explained by the highly mobile SiO_2 atoms on the surface, which are limited by their ability to find a preferential site upon which to attach. Slower growth would then favor homogeneous nucleation of the SiO_2 phase, rather than attachment to existing regions of SiO_2.

IV. Conclusion

This study showed that the sputtering deposition rate can greatly affect the microstructure that forms during metal–oxide phase separation in magnetic media.

By time-dependence measurement and calculation, the research results showed that, although the visual SiO_2 network appeared to be complete (with a 5-nm small grain size), the actual grains remained exchange coupled. This was also consistent with the observations from the high-resolution cross-sectional TEM images.

If we lower the deposition rate from 0.28 to 0.05 nm/s as in Media II, the lower rate resulted in a better defined oxide network, but the morphology of the CoCrPt grains became spherical instead of columnar. This might be due to the driving force of interfacial energy minimization and the lower deposition rate drove the system more toward the equilibrium, and/or kinetics that favored homogeneous renucleation of SiO_2 at slower rates.

Acknowledgment

This work was supported by the Imation Corporation under NIST ATP Award 70NANB2H3040, and by the Data Storage Systems Center of Carnegie Mellon University. The authors would like to thank Dr. C. Park for helpful discussions.

References

[1] T. Oikawa, M. Nakamura, H. Uwazumi, T. Shimats, H. Muraoka, and Y. Nakamura, "Microstructure and magnetic properties of CoPtCr-SiO_2 perpendicular recording media," *IEEE Trans. Magn.*, vol. 38, no. 5, pp. 1976–1978, Sep. 2002.

[2] M. P. Sharrock, "Recent advances in metal particulate recording media: Toward the ultimate particle," *IEEE Trans. Magn.*, vol. 36, no. 5, pp. 2420–2425, Sep. 2000.

[3] M. P. Sharrock, "Measurement and interpretation of magnetic time effects in recording media," *IEEE Trans. Magn.*, vol. 35, no. 6, pp. 4414–4422, Nov. 1999.

[4] T. Shimatsu, H. Sato, T. Oikawa, Y. Inaba, O. Kitakami, S. Okamoto, H. Aoi, H. Muraoka, and Y. Nakamura, "High-potential magnetic anisotropy of CoPtCr-SiO_2 perpendicular recording media," *IEEE Trans. Magn.*, vol. 41, no. 2, pp. 556–571, Feb. 2005.

[5] H.-S. Lee, L. Wang, J. A. Bain, and D. E. Laughlin, "Thin-film recording media on flexible substrates for tape applications," *IEEE Trans. Magn.*, vol. 41, no. 2, pp. 654–659, Feb. 2005.

[6] D. L. Smith, *Thin-Film Deposition: Principles and Practice*. New York: McGraw-Hill, 1995, pp. 136–139.

Manuscript received March 13, 2006 (e-mail: linwang@cmu.edu).